BIOCHEMICAL AND BIOPHYSICAL RESEARCH COMMUNICATIONS **238,** 599–605 (1997)
ARTICLE NO. RC977337

Oligomerization of Expanded-Polyglutamine Domain Fluorescent Fusion Proteins in Cultured Mammalian Cells

Osamu Onodera,* James R. Burke,*,† Sara E. Miller,‡ Susan Hester,‡ Shoji Tsuji,§ Allen D. Roses,*,†,¶ and Warren J. Strittmatter*,†,¶,[1]

**Department of Medicine (Neurology), ‡Department of Microbiology, ¶Department of Neurobiology, and †Deane Laboratory, Duke University Medical Center, Durham, North Carolina 27710; and §Department of Neurology, Brain Research Institute, Niigata University, Niigata 951, Japan*

Received August 15, 1997

Six inherited neurologic diseases, including Huntington's disease, result from the expansion of a CAG domain of the disease genes to produce a domain of more than 40 glutamines in the expressed protein. The mechanism by which expansion of this polyglutamine domain causes disease is unknown. Recent studies demonstrated oligomerization of polyglutamine-domain proteins in mammalian neurons. To study oligomerization of polyglutamine proteins and to identify heterologous protein interactions, varying length polyglutamine-green fluorescent protein fusion proteins were expressed in cultured COS-7 cells. The 19- and 35-glutamine fusion proteins (non-pathologic length) distributed diffusely throughout the cytoplasm. In contrast, 56- and 80-glutamine fusion proteins (pathologic length) formed fibrillar arrays resembling those previously observed in neurons in Huntington's disease and in a transgenic mouse model. These aggregates were intranuclear and intracytoplasmic. Intracytoplasmic aggregates were surrounded by collapsed intermediate filaments. The intermediate filament protein vimentin co-immunoisolated with expanded polyglutamine fusion proteins. This cellular model will expedite investigations into oligomerization of polyglutamine proteins and their interactions with other proteins.

Six inherited neurodegenerative diseases are caused by expanded CAG repeats (>40) in the disease-producing genes. The CAG repeat encodes a polyglutamine domain in the expressed proteins (1-4). These diseases, Huntington's disease (HD), dentatorubral pallidoluysian atrophy (DRPLA), spinocerebellar atrophy 1 and 2 (SCA 1 and 2), spinobulbar muscular atrophy (SBMA), and Machado-Joseph disease (MJD) share common molecular, cellular, and clinical features. They are dominantly inherited diseases, except X-linked SBMA, producing progressive motor control disturbances, with pathology limited to select populations of neurons in the central nervous system.

Several observations suggest that the polyglutamine domain of these proteins is itself critical in disease pathogenesis. For each of these diseases, expression of protein with a polyglutamine domain less than 35 glutamines is associated with a normal phenotype, greater than 40 glutamines causes disease. Increasing the size of the polyglutamine domain causes earlier age-of-onset and more severe clinical manifestations (1-4). These six proteins have no sequence homology other than the polyglutamine domain (1-4). Although the size of the polyglutamine domain in these proteins appears to determine critical intracellular interactions producing either a normal or a disease phenotype, the mechanism of toxicity of expanded polyglutamine proteins is unknown.

Perutz et al. proposed that polyglutamine domains may self-associate by anti-parallel packing to form β-pleated sheets and thereby oligomerize proteins (5). Biophysical studies, molecular modeling, and electron- and X-ray microscopy demonstrated that synthetic polyglutamine peptides produced anti-parallel β-sheets (5). Perutz hypothesized that a glutamine domain of a protein may bind with other proteins and demonstrated that incorporation of a polyglutamine domain into a monomeric protein caused its di- and trimerization *in vitro* (6). To study polyglutamine protein oligomerization within the native intracellular environment, and to identify potential heterologous protein interactions, we transfected mammalian COS-7 cells to express varying length polyglutamine domain- green fluorescent fusion proteins. In this study we demonstrate that long polyglutamine fusion proteins (glutamine domains > 40) oligomerize in COS-7 cells in a

[1] To whom correspondence should be addressed. Fax: (919) 684-6514. E-mail: warren@neuro.duke.edu.

0006-291X/97 $25.00

length- and time-dependent manner, while shorter fusion proteins do not. The fusion protein aggregates resemble aggregates in cortical neurons in Huntington's disease and in a transgenic mouse model. In addition, we show that the cytoplasmic fusion proteins aggregate on intermediate filaments and cause their collapse. This demonstration of length-dependent oligomerization of polyglutamine domain proteins in cultured mammalian cells, and the identification of their interactions with other molecules will facilitate studies on the mechanisms critical in disease pathogenesis.

MATERIALS AND METHODS

Construction of polyglutamine clones. Polyglutamine-GFP fusion proteins were synthesized by PCR from the human DRPLA cDNA. Each clone is denoted Q followed by the number of uninterrupted glutamines. DRPLA cDNA containing 79 or 14 CAG repeats was used as a template to construct clones Q80-GFP and Q19-GFP using primers 5CEu: 5′TGATCTCGAGCGCCACCATGGTCTCAACAC-ATCACCATCACCAC and 3NEu3: 5′ TGATGAATTCGAGGGGGC-CCAGAGTTTCCGTG (7). For construction of Q56-GFP and Q35-GFP, we used TA55 and Q35 plasmid DNA (8). The PCR was performed as previously described (8). Fragments were cloned into the *Xho* I and *EcoR* I site of the pEGFP-N1 vector (Clontech, Palo Alto, CA). The nucleotide sequences of all constructs were confirmed by the dideoxynucleotide chain terminator method.

The amino-acid sequence of each clone was: Q10 to Q80: MVSTHH-HHH (Q)19-80HHGNSGPPRIVQSTVPRARDPPVAT-GFP. The underlined sequence represents the sequence of the multi-cloning site of pEGFP-N1.

Cell culture and transfection. COS-7 cells were maintained in Dulbecco's modified Eagles's medium (DMEM) supplemented with 10% fetal calf serum (FCS). The transfection was performed by using lipofectamine reagent according to the protocol from GIBCO BRL (Gaithersburg, MD). Purified DNA was prepared using QIAGEN-tips columns (Qiagen, Chatsworth, CA). Cells were examined under phase and fluorescence microscopy. The percentage of cells with visible aggregates of fusion protein were determined by counting cells with visible aggregates, divided by the total number of cells with green fluorescence 72 hours after transfection, in two independent experiments. In each series more than 500 transfected cells were counted. For anti-microtubule drug treatment, cells were grown on Lab-Tek 4 Chamber Slide (Nunc Inc, Naperville, Illinois) and transfected. 24 hr after transfection, the media was changed to DMEM supplemented with 10% FCS and 10 μg/ml nocodazole (diluted from 1 mg/ml solution made in DMSO) for 5 hr.

Immunofluorescence microscopy and image analysis. For immunofluorescent labeling, cells grown and transfected on chamber slides were either fixed in freshly made 4% paraformaldehyde in PBS (pH 7.3) or in methanol at −20°C. After fixation, cell were washed in TBST (0.15M NaCl, 0.02M Tris-HCl (pH 7.4), 0.1% Triton X-100) and then incubated in 2% BSA at room temperature for 10 min. Cells were incubated with primary antibodies at room temperature for 30-90 min, extensively rinsed in TBST, and exposed to secondary fluorescent antibodies at room temperature for 30 min. After repeated rinses in TBST, cells were treated with Vectashield mounting media (Vector Laboratories, Burlingame, CA). The following immunoreagents were used: monoclonal antibodies to vimentin (V9) (Boehringer-Mannheim, Indianapolis, IN), β-tubulin (Amersham International, Buckinghamshire, England), actin (AC-40) (Sigma BioSciences, St. Louis, MO); Texas red-labeled horse anti-mouse IgG (H + L) (Vector Laboratories). Images were obtained using a Zeiss microscope equipped with fluorescein and rhodamine filter sets and Zeiss 32× lens (Carl Zeiss, Inc., Thornwood, NY). The images were either photographed directly on Kodak Ektachrome p1600 film (exposure 4 s to 30 s). Confocal images were obtained using Bio-Rad MRC-600 Confocal System (Bio-Rad Labs, Richmond, CA) with an argon laser and Nikon Diaphot microscope equipped with a Nikon 60× oil immersion objective. Hard copies of stored images were obtained from Adobe Photoshop files.

Electron microscopy. Cells were fixed in 4% paraformaldehyde in PIPES (piperazine-N,N′-bis (2-ethanesulfonic acid)) buffer, pH 7.0; infiltrated with 2.1 M sucrose in phosphate buffered saline (PBS), 3 changes in 30 minutes; placed on cryo stubs; and snap frozen and stored until use in liquid nitrogen. Ultrathin cryosections were cut on a Reichert-Jung Ultracut E ultramicrotome equipped with an FC-4E cryochamber (Leica, Deerfield, IL). They were collected on loops with 2.3 M sucrose in PBS, placed onto Formvar- and carbon-coated copper-rhodium grids, and treated 30 minutes with 5% FCS in PBS to block nonspecific staining. Incubation with primary antibody was for 1 hour at room temperature; mouse monoclonal anti-GFP (Clontech) used at 1:50. Grids were extensively washed (6 changes in 30 minutes) with PBS and then incubated with secondary antibodies for 30 minutes at room temperature. Secondary antibodies were goat anti-mouse IgG conjugated to10 nm colloidal gold (Amersham Life Sciences). The antibody dilutions were made in 5% FCS in PBS. Gold-labeled probes were diluted 1:10 and reacted for 30 minutes at room temperature. After extensive PBS washing as before, grids were rinsed in 3 drops of water and incubated on drops of 2 M methyl cellulose containing saturated aqueous uranyl acetate (9 parts to 2 parts). They were then drained on filter paper, air dried, and viewed in a Philips EM300 electron microscope (Philips Electronic Inst. Co., Mahwah, N.J.).

Protein analysis. Each well of a 6-well plate was scraped and centrifuged and the cell pellet collected. The cell pellet was suspended in Laemmli buffer containing 2% SDS and 5% β-mercaptoethanol and boiled for 3 min. The samples were electophoresed on a 10% polyacrylamide gel containing 2% SDS. Proteins were transferred to Immobilon P membrane (Milipore, Bedford, MA) by standard Western transfer techniques. Proteins were transferred and immunoblotted as previously described (8).

Co-immunoisolation of polyglutamine domain fusion proteins and vimentin. Q19, Q56 and Q80-GFP clones were digested by *Xho* I and *BsrG* I and fragments were cloned into *Xho* I and *Asp*718 I site of pcDNA3.1 (−)/Myc-His C vector (Invitrogen, San Diego, CA). Clones were named Q19-Myc, Q56-Myc and Q80-Myc respectively. COS-7 cells were transfected with Q19-Myc, Q56-Myc or Q80-Myc expression plasmids in 6 well plates. 48 hours after transfection, the cells were rinsed with PBS, then preincubated 30 min with 0.5 ml extraction buffer (100 mM KCl, 10 mM 1,4-piperazinediethane sulfonic acid [PIPES], pH 6.8, 300 mM sucrose, 2 mM $MgCl_2$, 1 mM EGTA and 0.5% Triton X-100 containing proteinase inhibitors (leupeptin 1 μg/ml, pepstatin 1 μg/ml, aprotinin 5 μg/ml and PMSF 1 mM) at 4°C (9). The cells maintained their morphology, and the aggregrated GFP-fusion protein was retained, but the nonaggregated fusion protein was reduced. The remaining material was incubated in 500 ml cell lysis buffer (50 mM Tris-HCl (pH 7.4) 150 mM NaCl, 5 mM EDTA, and 1% Triton X-100) with proteinase inhibitors for 30 min. The cells were scraped with a rubber policeman and centrifuged 5000 rpm for 3 min at 4°C. The supernatant was filtered with a 0.65 μm Ultra-free-MC (Milipore) and incubated with 2 μl anti-Myc mouse monoclonal antibody (Invitrogene) for 16 hours at 4°C. 50 μl DYNABEADS (M-450) sheep anti-mouse IgG (DYNAL, Lake Success, NY) were washed twice with binding buffer (TrisHCl (pH 7.4) 20 mM, NaCl 150 mM and 2% dried milk) and suspended in 500 μl binding buffer containing proteinase inhibitors. 500 μl of suspended beads were added to each sample and incubated 2 hours at 4°C. After incubation Dynabeads were separated by a magnetic separation unit and intensively washed three times with washing buffer (Tris-HCl (pH 7.4) 20 mM, NaCl 150 mM and 0.5 % Triton X-100). Washed beads were boiled 5 min in Laemmli buffer containing

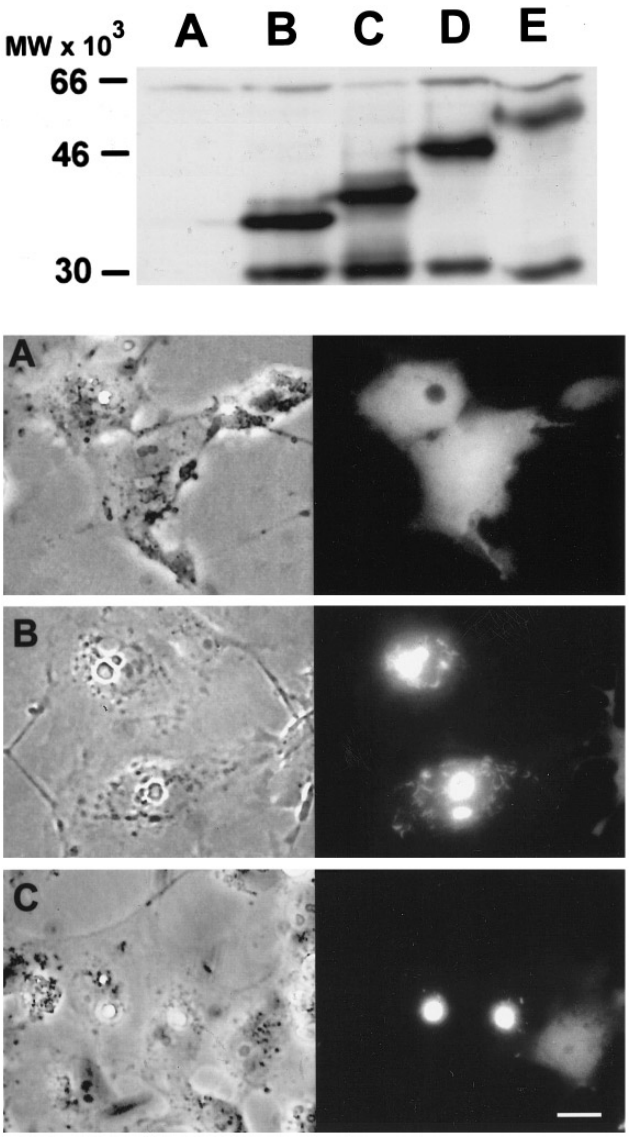

FIG. 1. (Top) Expression of Polyglutamine (Q)-GFP Fusion Proteins in COS-7 Cells. Lane A, non-transfected COS-7 cells; Lane B, Q19-GFP; Lane C, Q35-GFP; Lane D, Q 56-GFP; Lane E, Q80-GFP. COS-7 cells were harvested and homogenized 24 hours after transfection. Following electrophoresis and Western transfer, proteins were detected with an anti-GFP antibody, as described in Materials and Methods. (Bottom) Phase Contrast and Fluorescence Microscopy of COS-7 Cells Expressing: A) Q19-GFP, B) Q56-GFP or C) Q80-GFP. Cells were examined 24 hours after transfection under phase contrast (left) or for GFP fluorescence (right). Bar is 20 μm.

6% SDS without β-mercaptoethanol, separated on the magnetic separator and 25 μl of the supernatant was subjected to 7.5% PAGE.

RESULTS

Expanded polyglutamine-GFP fusion proteins oligomerize in cultured mammalian cells. Transiently transfected COS-7 cells produced fusion proteins containing the polyglutamine domain and GFP (Figure 1 TOP). Each fusion protein is denoted Q followed by the number of uninterrupted glutamines. Approximately equal amounts of polyglutamine-GFP fusion proteins were translated in each of the transfected cell cultures.

Cells expressing polyglutamine domain-GFP fusion proteins were examined by phase contrast (Figure 1 BOTTOM, Left Panel), and fluorescence microscopy (Figure 1 BOTTOM, Right Panel). 24 hours after transfection the 19-glutamine-GFP fusion protein (Q19-GFP) and the 35-glutamine-GFP fusion protein (Q35-GFP) were diffusely and uniformly distributed throughout the cytoplasm (Figure 1A shows Q19-GFP). In contrast, the 56-glutamine-GFP fusion protein (Q56-GFP) formed both multiple small aggregates throughout the cytoplasm and large aggregates adjacent to the nucleus (Figure 1B). The 80-glutamine-GFP fusion protein (Q80-GFP) produced large perinuclear fluorescent aggregates (Figure 1C). Q80-GFP initially distributed diffusely, but within18 hours formed small aggregates adjacent to the nucleus and within 24 hours formed large perinuclear aggregates, with disappearance of the diffuse cytoplasmic fluorescence.

The percentage of cells with aggregates of fluorescent protein were assayed 72 hours after transfection (see Material and methods). The percentage of cells with fluorescent aggregates dramatically increased when the length of poly-glutamine was greater than 40. Q19-GFP and Q35-GFP produced few aggregates (1.77 % $\pm$ 0.56 (Mean $\pm$ SE), 3.75% $\pm$ 0.06, respectively), while Q56-GFP and Q80-GFP formed abundant aggregates (45.7 % $\pm$ 1.30, 61.8 % $\pm$ 0.16, respectively).

Expanded polyglutamine fusion proteins form fibrous aggregates. The morphology of the Q80-GFP aggregates was further defined by electron microscopy of immunogold-labeled proteins. The perinuclear aggregate of Q80-GFP is a mesh of fibrillar protein (Figure 2A) which contains abundant immunoreactive GFP (Figure 2B). No membranous structure was detected around the fibrillar protein aggregate. Similar GFP-immunoreactive aggregates were also observed in the nuclei (data not shown). No aggregates were identified in Q19-GFP transfected cells (data not shown).

Over-expression of pathologic-length polyglutamine fusion protein collapses the intermediate filament network. Large aggregates of Q56-GFP and Q80-GFP were often located near the nucleus and Golgi apparatus. Small aggregates of Q56-GFP were distributed throughout the cytoplasm. Since both the intermediate filament (IF) network and microtubule network originate near the Golgi and project throughout the cytoplasm, we investigated the relationship of fusion protein aggregates with the cytoskeleton (10, 11). The normal IF network extends from the center of the cell near the nucleus to the cell periphery. The IF network appeared the same in Q19-GFP transfected cells and in non-transfected cells (Figure 3 A). In Q56-GFP trans-

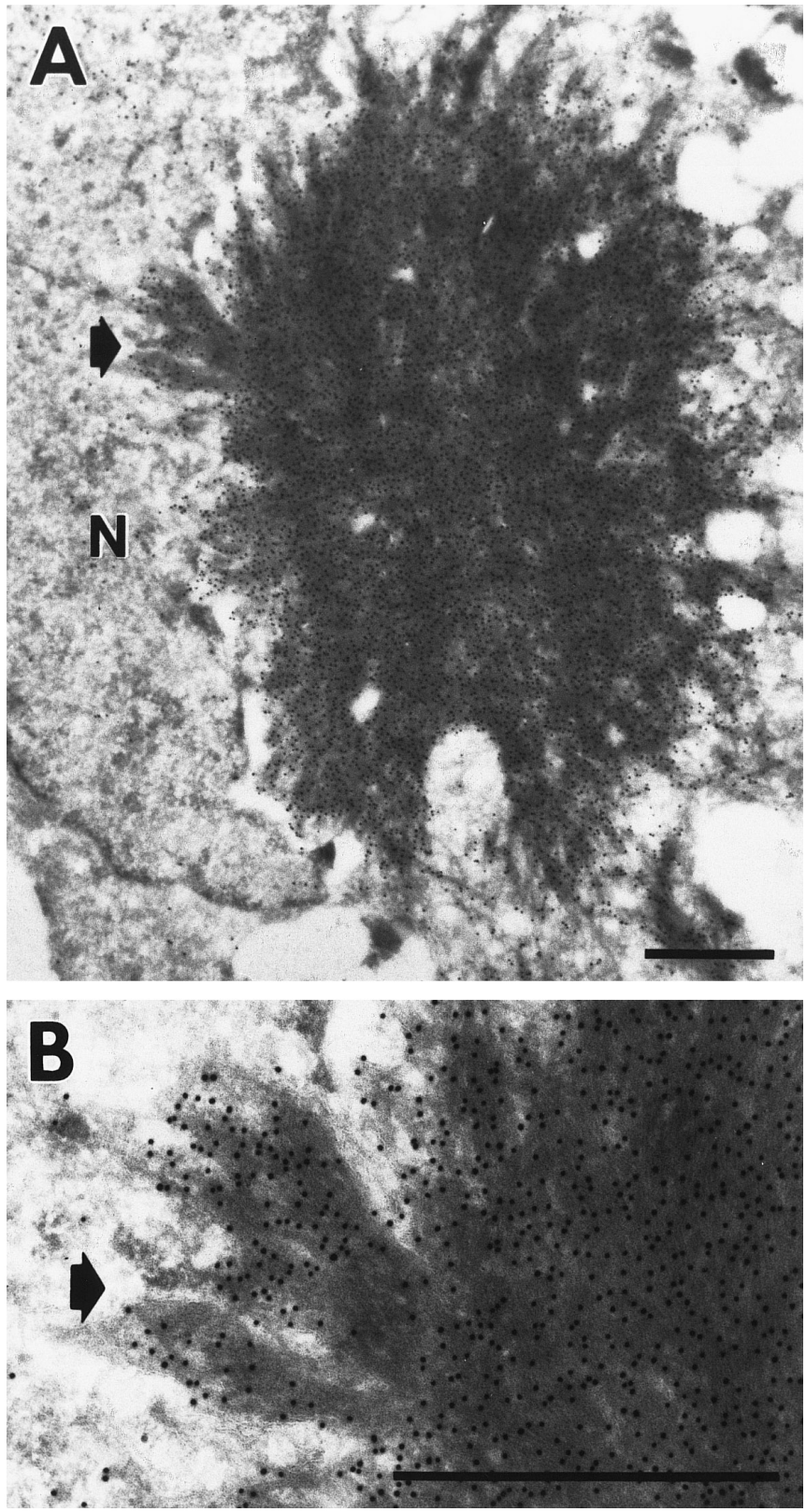

FIG. 2. Ultrastructure of aggregated Q80-GFP in COS-7 cells. 24 hours after transfection, COS-7 cells producing Q80-GFP were processed for ultracryotomy and immunogold labeling. (A) Low magnification electron micrograph of a large fibrillary inclusion, incubated with anti-GFP antibody followed by secondary antibody conjugated to10 nm gold particles. (N is nucleus.) (B) Higher magnification of fibrillar arm at arrow in A, showing heavy anti-GFP immunogold labelling of strands. Bars are 1 μm.

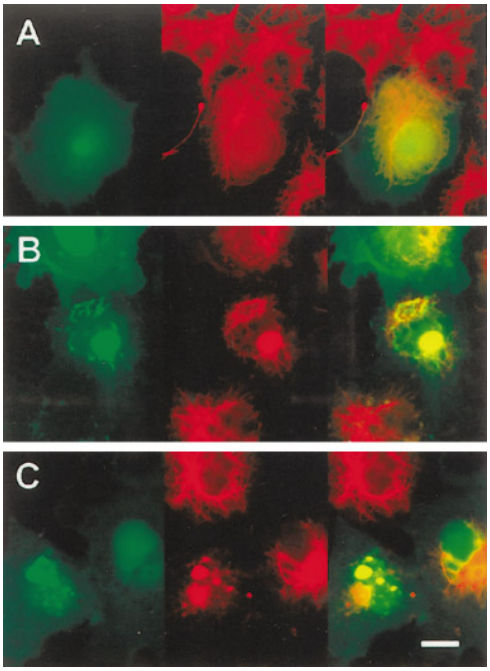

FIG. 3. Localization of Polyglutamine-GFP Fusion Proteins and Vimentin. Cells expressing (A) Q19-GFP; (B) Q56-GFP; or (C) Q80-GFP were fixed 24 hours after transfection, and incubated with an anti-vimentin antibody (V9). The cells were examined under confocal microscopy for GFP, using FITC optics (left), for anti-vimentin, using Texas red optics (middle), or two color overlay of the GFP and vimentin pattern (right). Bar is 20 μm.

fected cells, small aggregates of fusion protein were associated primarily with the IF network (Figure 3 B). These clustered aggregates of fusion protein disrupted the uniform distribution of the IF array and collapsed the IF network around the nucleus and around the fusion protein aggregate, as shown in the center cell. Even after disruption of the microtubule array by nocodazole, aggregates of Q56-GFP still co-localized with the IF network (data not shown). Q80-GFP produced large perinuclear aggregates, with severe disruption of the IF network and collapse adjacent to the nucleus (Figure 3 C). In these cells the IFs no longer extended to the cell membrane. Adjacent non-transfected cells demonstrated normal IF network morphology. In contrast to the disrupted IF network, the microtubule network was intact. No association of Q80-GFP was observed with the actin network (not shown).

Vimentin coimmunoisolates with long polyglutamine fusion proteins. The spatial association of aggregated Q56-GFP or Q80-GFP with intermediate filaments does not prove direct molecular interaction. To determine whether long polyglutamine proteins bind intermediate filaments, we immunoisolated polyglutamine domain proteins from COS-7 cells expressing Q19-Myc, Q56-Myc or Q80-Myc. As shown in Figure 4, vimentin coimmunoisolated with the 56- and 80-polyglutamine fusion proteins, but not with the 19- polyglutamine protein. In contrast, β-tubulin did not coimmunoisolate (not shown). These observations provide additional support for the conclusion that expanded polyglutamine domain fusion proteins bind intermediate filaments.

DISCUSSION

Polyglutamine protein aggregation appears important in the pathogenesis of the CAG-repeat diseases. Electron microscopic examination of Huntington's disease neurons demonstrate cytoplasmic and nuclear protein aggregates (12, 13). Both the nuclear and cytoplasmic aggregates are fibrillar structures similar to the fibrillar arrays observed by us in COS-7 cells (12, 13). As shown by Scherzinger et al, a GST- fusion protein of exon 1 of huntingtin with an expanded CAG repeat domain, produced by *E. coli*, forms similar protein aggregates *in vitro* (14). Ikeda et al. reported punctate intracytoplasmic distribution of a truncated MJD1 protein with an expanded polyglutamine domain (15). Here we demonstrate that expanded polyglutamine-domain proteins aggregate in cultured mammalian

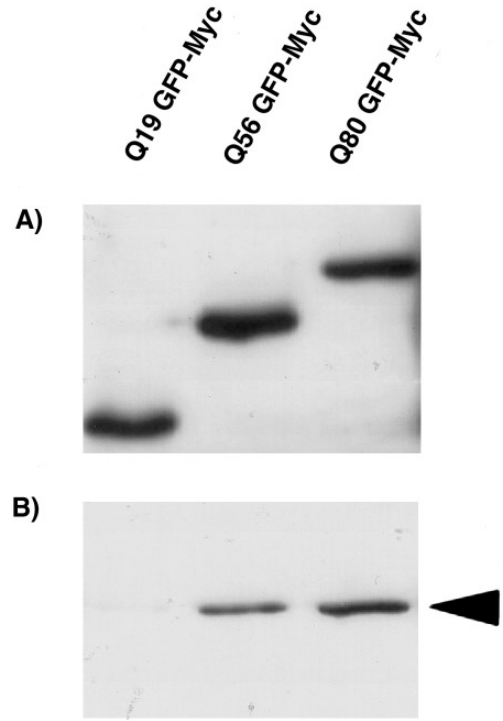

FIG. 4. Immunoisolation of polyQ-Myc fusion proteins and vimentin. Cells expressing Q19-Myc, Q56-Myc or Q80-Myc were lysed and immunoprecipitated with an anti-Myc antibody and separated by secondary antibody coated beads. Binding materials were eluted and analyzed by SDS-PAGE under non-reducing conditions, and immunoblotted with an anti-vimentin monoclonal antibody (V9) (B). The same filters reprobed with an anti-GFP antibody (A). Arrowhead: Vimentin.

cells in a length-dependent manner, forming cytoplasmic and nuclear oligomeric structures similar to those seen in diseased neurons.

The intracellular compartmentalization of the CAG-triplet repeat disease proteins has been examined. All of these polyglutamine-domain proteins are cytoplasmic except for ataxin-1 in SCA-1 (2, 16-20). The ataxin -1 protein with a normal polyglutamine domain is primarily nuclear, but is in the cytoplasm of affected Purkinje cells (18). Huntingtin is a cytoplasmic protein associated with synaptic vesicles. Davies et al. recently demonstrated that neurons of mice transgenic for exon 1 of the human Huntington's gene with 115 to 156 CAG expansions had intranuclear inclusions (21). Since inclusions in Huntington disease neurons are both intracytoplasmic and intranuclear, expanded-huntingtin must be distributed into both intracellular compartments.

The mechanism of length-dependent oligomerization of polyglutamine domain proteins is unknown. Our results suggest that expanded polyglutamine domains adopt a novel secondary structure which promotes oligomerization and determines interactions with other proteins. Supporting this hypothesis, Trottier et al. have identified an antibody which binds only pathologic length polyglutamine proteins (22). Length-dependent polyglutamine protein interactions with other proteins have been previously shown, either *in vitro* or in the yeast two hybrid system, for glyceraldehyde-3-phosphate dehydrogenase (23), HAP1 (24), HIP1 (25, 26) and apopain (27).

Perutz et al. demonstrated that synthetic polyglutamine peptides self-assemble into antiparallel β-pleated sheets *in vitro,* and showed that a polyglutamine domain of a protein can dimerize protein (5, 6). The fibrillar aggregates of Q80-GFP we observed by electron microscopy (Figure 2) may also arise from assembly of β-sheet arrays. Perutz also speculated that expansion of polyglutamine beyond a critical number promotes oligomerization (28). The dramatic differences in oligomerization between Q35-GFP and Q56-GFP in our experiments support this hypothesis and is consistent with the clinical observation that polyglutamine domains greater than 40 is associated with disease.

The intracellular distribution of the polyglutamine fusion protein aggregates suggests interaction with the IF network. This interaction with intermediate filaments is preserved even after disruption of microtubules. Vimentin, which forms the intermediate filaments, co-immunoisolates with polyglutamine in a length dependent manner, while β-tubulin does not.

The specific molecular interaction between polyglutamine and intermediate filaments is not known. Aggregated polyglutamine-fusion protein may directly bind vimentin, which forms the IF, or bind other proteins associated with the IF network. Mature neurons, unlike COS-7 cells, do not express vimentin, but produce homologous intermediate filament proteins, neurofilament. Vimentin and neurofilament proteins are homologous at the primary, secondary, and tertiary structural levels (for review see (29)). Expanded polyglutamine domain proteins may interact with neurofilaments, similar to their interactions with IFs of COS-7 cells. The production of oligomerized GFP-polyglutamine fusion protein in cultured mammalian cells which mimic the aggregates seen in Huntingtons disease neurons should facilitate studies examining the mechanism of oligomerization, their interactions with other proteins in the cell, and the identification of compounds which inhibit these protein-protein interactions.

ACKNOWLEDGMENTS

We are grateful to Margaret Martin for technical assistance. We thank Larry Hawkey for assistance with confocal microscopy, William Matthew for assistance with fluorescence microscopy, and Michael Sheetz for helpful discussion. This work was supported by NCI 5-P30-CA-14236-24 to S.M.

REFERENCES

1. Imbert, G., Saudou, F., Yvert, G., Devys, D., Trottier, Y., Garnier, J. M., Weber, C., Mandel, J. L., Cancel, G., Abbas, N., Durr, A., Didierjean, O., Stevanin, G., Agid, Y., and Brice, A. (1996) *Nature Genet.* **14,** 285–291.
2. Paulson, H. L., and Fischbeck, K. H. (1996) *Annu. Rev. Neurosci.* **19,** 79–107.
3. Pulst, S. M., Nechiporuk, A., Nechiporuk, T., Gispert, S., Chen, X. N., Lopes-Cendes, I., Pearlman, S., Starkman, S., Orozco-Diaz, G., Lunkes, A., DeJong, P., Rouleau, G. A., Auburger, G., Korenberg, J. R., Figueroa, C., and Sahba, S. (1996) *Nature Genet.* **14,** 269–276.
4. Sanpei, K., Takano, H., Igarashi, S., Sato, T., Oyake, M., Sasaki, H., Wakisaka, A., Tashiro, K., Ishida, Y., Ikeuchi, T., Koide, R., Saito, M., Sato, A., Tanaka, T., Hanyu, S., Takiyama, Y., Nishizawa, M., Shimizu, N., Nomura, Y., Segawa, M., Iwabuchi, K., Eguchi, I., Tanaka, H., Takahashi, H., and Tsuji, S. (1996) *Nature Genet.* **14,** 277–284.
5. Perutz, M. F., Johnson, T., Suzuki, M., and Finch, J. T. (1994) *Proc. Natl. Acad. Sci. U.S.A.* **91,** 5355–5358.
6. Stott, K., Blackburn, J. M., Butler, P. J., and Perutz, M. (1995) *Proc. Natl. Acad. Sci. U.S.A.* **92,** 6509–6513.
7. Onodera, O., Oyake, M., Takano, H., Ikeuchi, T., Igarashi, S., and Tsuji, S. (1995) *Am J Hum Genet* **57,** 1050–60.
8. Onodera, O., Roses, A. D., Tsuji, S., Vance, J. M., Strittmatter, W. J., and Burke, J. R. (1996) *FEBS Letters* **399,** 135–139.
9. L'Ecuyer, T. J., and Fulton, A. B. (1993) *Biotechniques* **14,** 436–41.
10. Trevor, K. T., McGuire, J. G., and Leonova, E. V. (1995) *J. Cell. Sci.* **108,** 343–356.
11. Cole, N. B., and Lippincott-Schwartz, J. (1995) *Curr. Opin. Cell Biol.* **7,** 55–64.
12. Roizin, L., Stellar, S., and Liu, J. C. (1979) *in* Advances in Neurology (Chase, T. N., Wexler, N. S., and Barbeau, A., Eds.), Vol. 23, pp. 95–122, Raven Press, New York.
13. Jackson, M., Gentleman, S., Lennox, G., Ward, L., Gray, T., Ran-

dall, K., Morrell, K., and Lowe, J. (1995) *Neuropathol Appl Neurobiol* **21,** 18–26.

14. Scherzinger, E., Lurz, R., Turmaine, M., Mangiarini, L., Hollenbach, B., Hasenbank, R., Bates, G. P., Davies, S. W., Lehrach, H., and Wanker, E. E. (1997) *Cell* **90,** 549–558.
15. Ikeda, H., Yamaguchi, M., Sugai, S., Aze, Y., Narumiya, S., and Kakizuka, A. (1996) *Nature Genet.* **13,** 196–202.
16. Gutekunst, C. A., Levey, A. I., Heilman, C. J., Whaley, W. L., Yi, H., Nash, N. R., Rees, H. D., Madden, J. J., and Hersch, S. M. (1995) *Proc Natl Acad Sci U S A* **92,** 8710–4.
17. Lumbroso, S., Sandillon, F., Georget, V., Lobaccaro, J. M., Brinkmann, A. O., Privat, A., and Sultan, C. (1996) *Eur J Endocrinol* **134,** 626–632.
18. Servadio, A., Koshy, B., Armstrong, D., Antalffy, B., Orr, H. T., and Zoghbi, H. Y. (1995) *Nat Genet* **10,** 94–8.
19. Trottier, Y., Devys, D., Imbert, G., Saudou, F., An, I., Lutz, Y., Weber, C., Agid, Y., Hirsch, E. C., and Mandel, J. L. (1995) *Nat Genet* **10,** 104–10.
20. Yazawa, I., Nukina, N., Hashida, H., Goto, J., Yamada, M., and Kanazawa, I. (1995) *Nat Genet* **10,** 99–103.
21. Davies, S. W., Turmaine, M., Cozens, B. A., DiFiglia, M., Sharp, A. H., Ross, C. A., Scherzinger, E., Wanker, E. E., Mangiarini, L., and Bates, G. P. (1997) *Cell* **90,** 537–548.
22. Trottier, Y., Lutz, Y., Stevanin, G., Imbert, G., Devys, D., Cancel, G., Saudou, F., Weber, C., David, G., Tora, L., Agid, Y., Brice, A., and Mandel, J. (1995) *Nature* **378,** 403–406.
23. Burke, J. R., Enghild, J. J., Martin, M. E., Jou, Y. S., Myers, R. M., Roses, A. D., Vance, J. M., and Strittmatter, W. J. (1996) *Nature Medicine* **2,** 347–350.
24. Li, X. J., Li, S. H., Sharp, A. H., Nucifora, F. C., Jr., Schilling, G., Lanahan, A., Worley, P., Snyder, S. H., and Ross, C. A. (1995) *Nature* **378,** 398–402.
25. Kalchman, M. A., Koide, H. B., McCutcheon, K., Graham, R. K., Nichol, K., Nishiyama, K., Kazemi-Esfarjani, P., Lynn, F. C., Wellington, C., Metzler, M., Goldberg, Y. P., Kanazawa, I., Gietz, R. D., and Hayden, M. R. (1997) *Nature Genetics* **16,** 44–53.
26. Wanker, E. E., Rovira, C., Scherzinger, E., Hasenbank, R., Walter, S., Tait, D., Colicelli, J., and Lehrach, H. (1997) *Human Molecular Genetics* **6,** 487–95.
27. Goldberg, Y. P., Nicholson, D. W., Rasper, D. M., Kalchman, M. A., Koide, H. B., Graham, R. K., Bromm, M., Kazemi-Esfarjani, P., Thornberry, N. A., Vaillancourt, J. P., and Hayden, M. R. (1996) *Nature Genetics* **13,** 442–9.
28. Perutz, M. F. (1996) *Curr Opin Struct Biol* **6,** 848–858.
29. Fuchs, E., and Weber, K. (1994) *Annu. Rev. Biochem.* **63,** 345–382.